Supplementary Information

Influence of Ancillary Ligands and Solvents on the Nuclearity of Ni-Ln complexes.

Jean-Pierre Costes,[a] , Sonia Mallet-Ladeira,[a] Laure Vendier,[a] Rémi Maurice,[b*] Wolfgang Wernsdorfer [c*]*

[a)] *LCC-CNRS, Université de Toulouse, CNRS, 31077 Toulouse, France*

[b)] *SUBATECH, UMR CNRS 6457, IN2P3/IMT Atlantique/Université de Nantes, Nantes, France*

[c)] *Institu Néel, CNRS, BP 166, 25 Avenue des Martyrs, 38042, Grenoble Cedex 9, France*

Keywords: Ni-Ln complexes; Coordination Chemistry; Structural determinations; Magnetic Properties; Zero-Field Splitting.

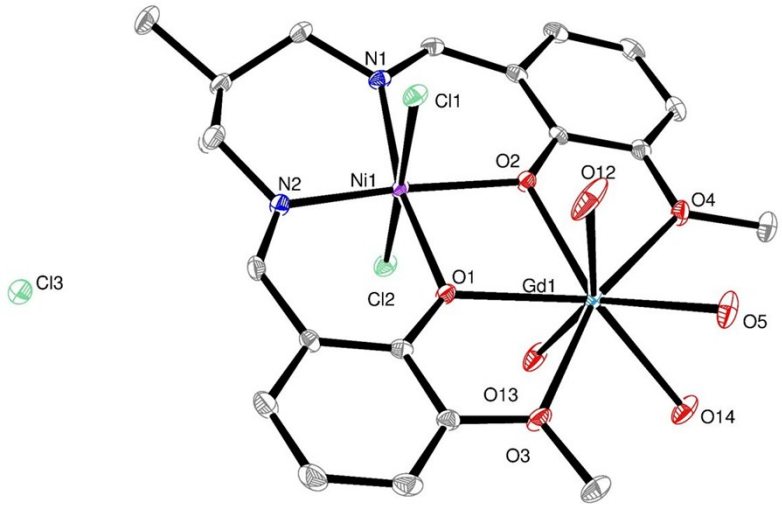

Figure S1. Plot of complex **2** with ellipsoids drawn at the 30 % probability level with partial atom numbering and H atoms omitted for clarity. Selected bond lengths (Å) and angles (°):Ni-N1 2.010(2), Ni-N2 2.014(2), Ni-O1 2.013(1), Ni-O2 2.031(1), Ni-Cl1 2.756(1), Ni-Cl2 2.5085(6), Gd-O1 2.330(1), Gd-O2 2.322(1), Gd-O3 2.452(2), Gd-O4 2.477(2), Gd-O5 2.388(2), Gd-O12 2.369(2), Gd-O13 2. 2.355(2), Gd-O14 2.418(1), Ni...Gd 3.5294(3) Å; Ni O1 Gd 108.50(6), Ni O2 Gd 108.18(6), O1 Gd O2 65.86(5)°.

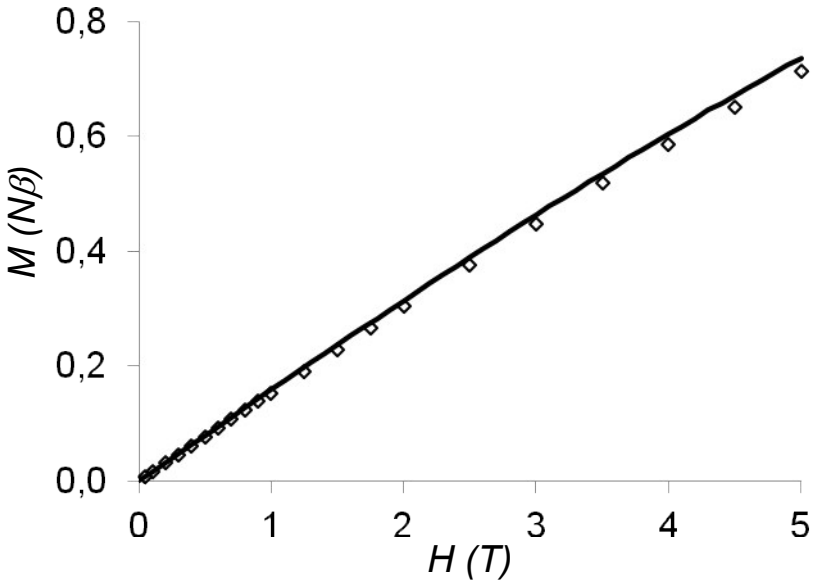

Figure S2. Field dependence of magnetization for complex **3**. The solid line corresponds to the best data fit (see the text).

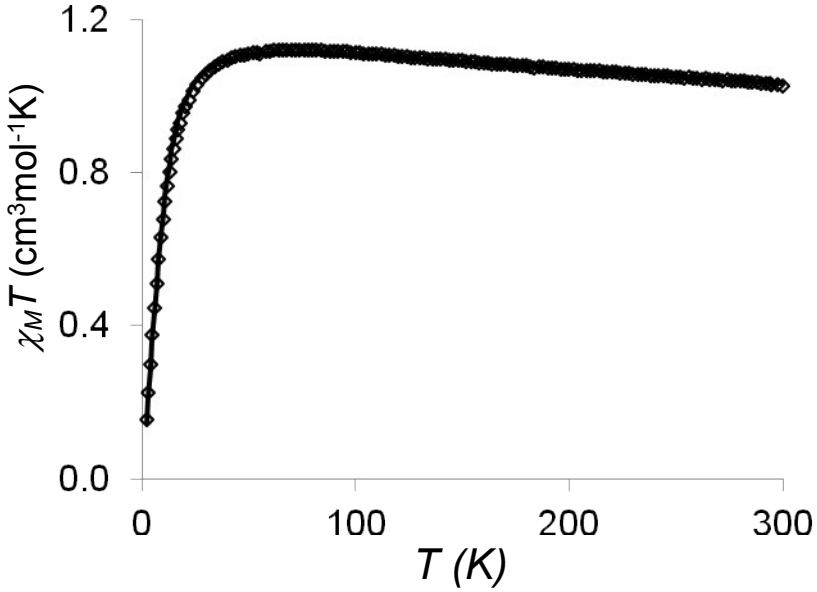

Figure S3. Temperature dependence of the $\chi_M T$ product for complex **8** at 0.1 T applied field. The solid line corresponds to the best data fit (see the text).

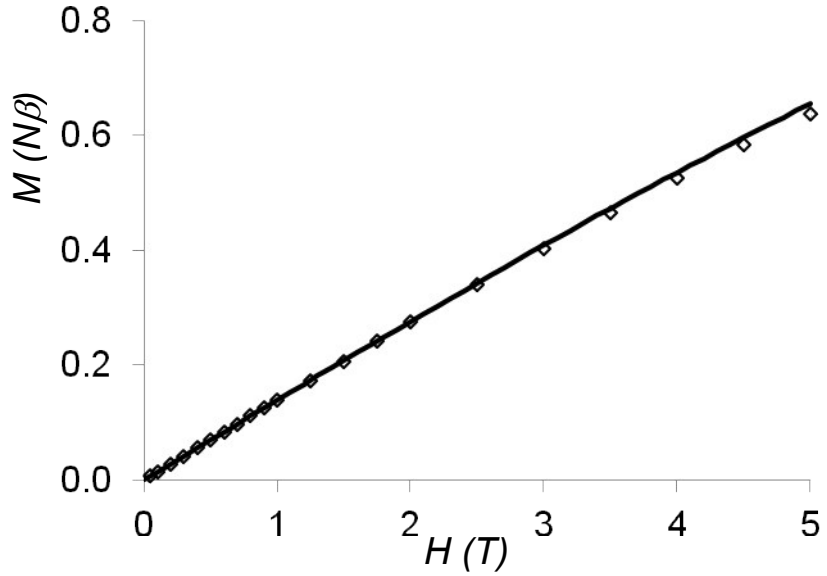

Figure S4. Field dependence of magnetization for complex **8**. The solid line corresponds to the best data fit (see the text).

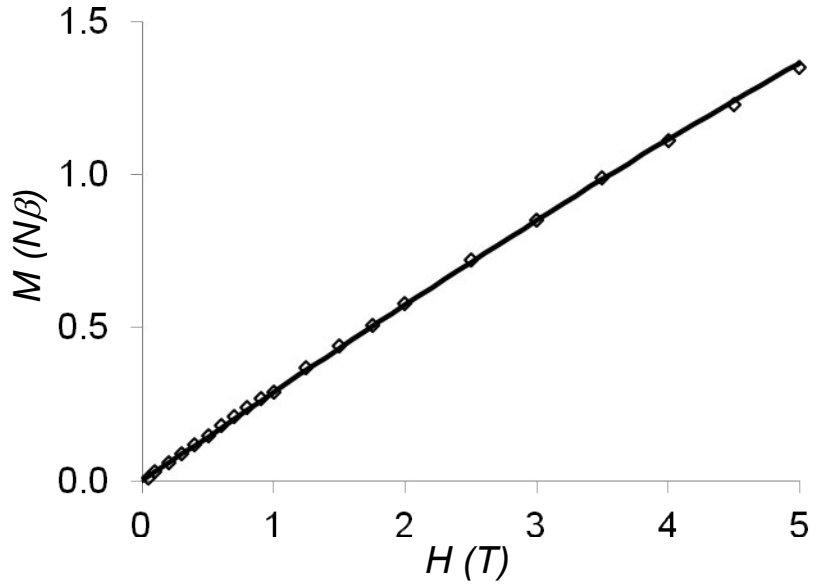

Figure S5. Field dependence of magnetization for complex **6** taking into account presence of an antiferromagnetic Ni-Ni interaction. The solid line corresponds to the best data fit (see the text).

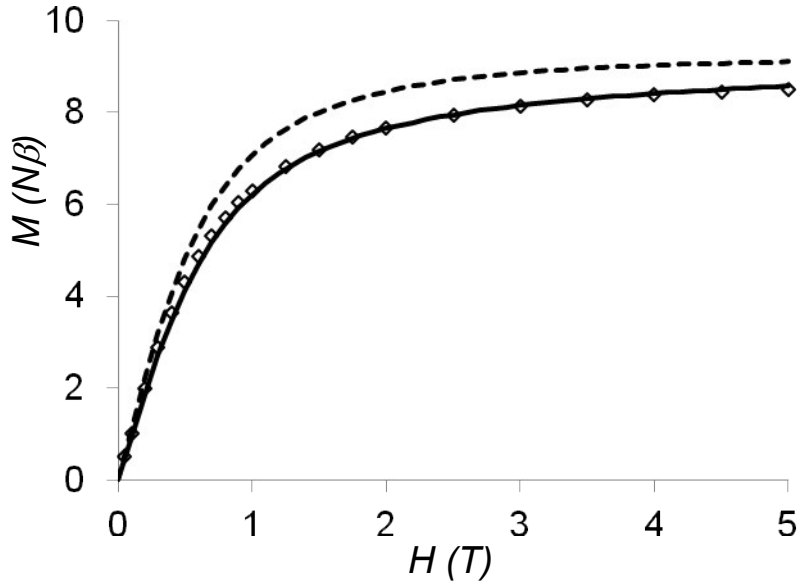

Figure S6. Field dependence of magnetization for complex **7** with (solid line) or without (dashed line) ZFS D_{Ni} parameter.

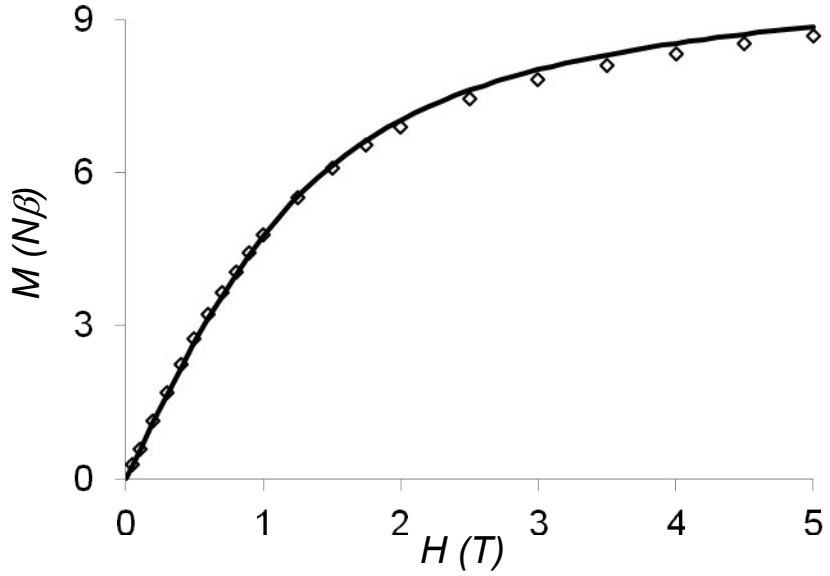

Figure S7. Field dependence of magnetization for complex **9**. The solid line corresponds to the best data fit (see the text).

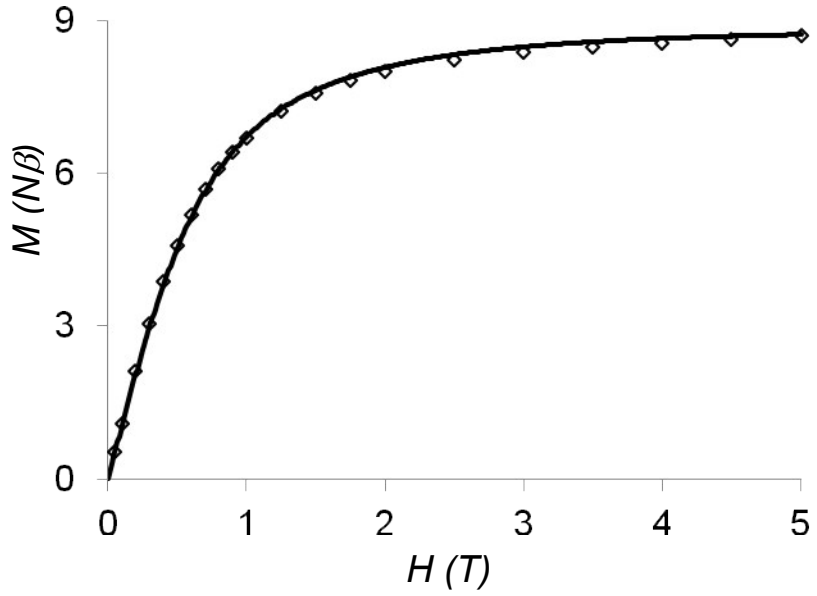

Figure S8. Field dependence of magnetization for complex **10**. The solid line corresponds to the best data fit (see the text).

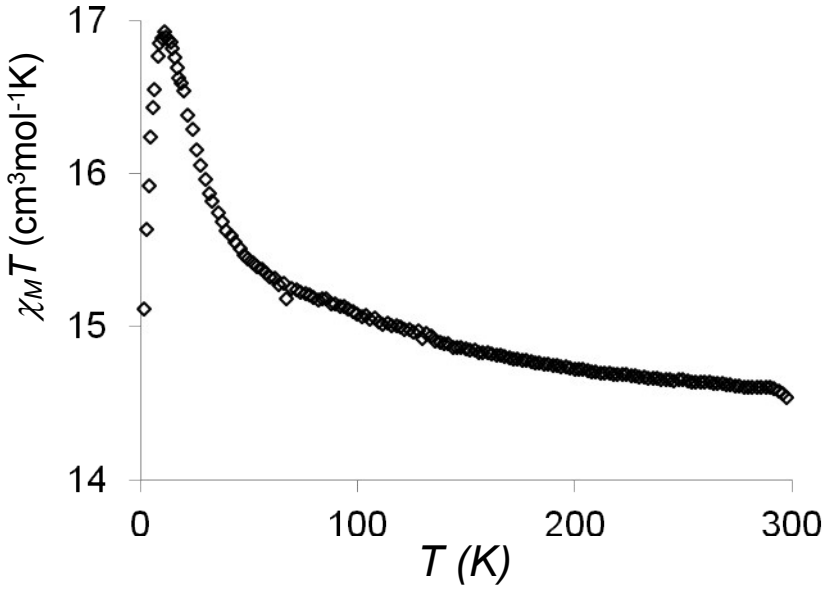

Figure S9. Temperature dependence of the $\chi_M T$ product for complex **4** at 0.1 T applied field.

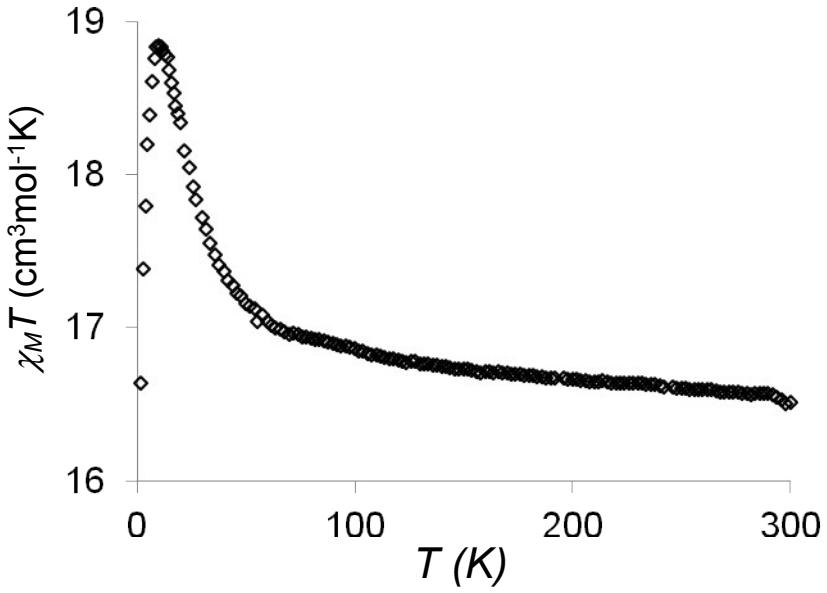

Figure S10. Temperature dependence of the $\chi_M T$ product for complex **5** at 0.1 T applied field.

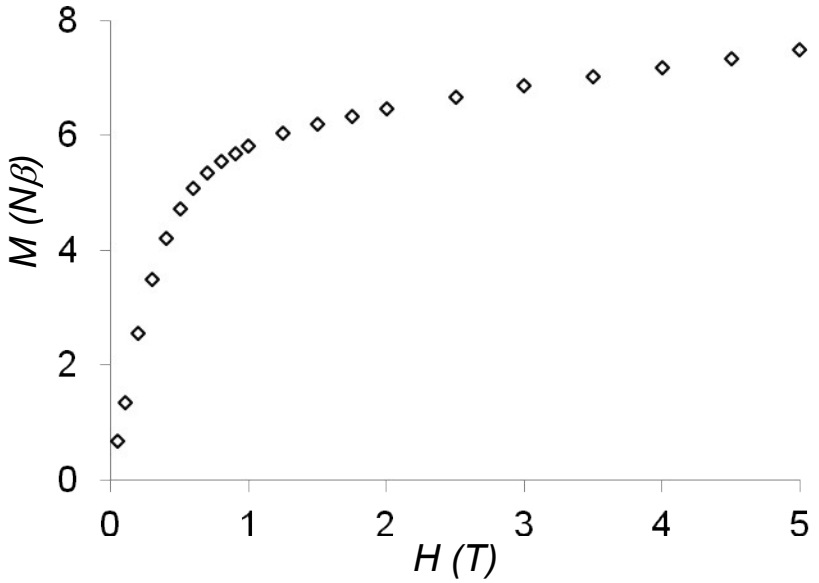

Figure S11. Field dependence of magnetization for complex **4**.

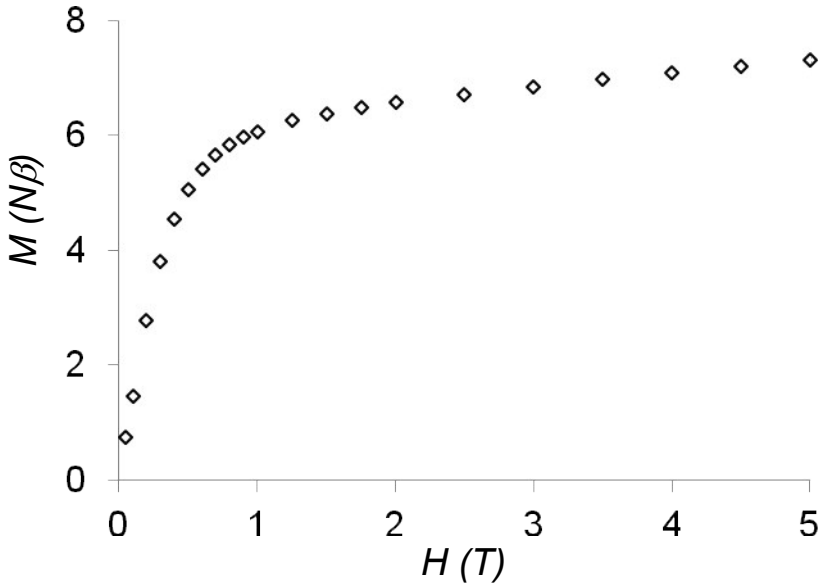

Figure S12. Field dependence of magnetization for complex **5**.

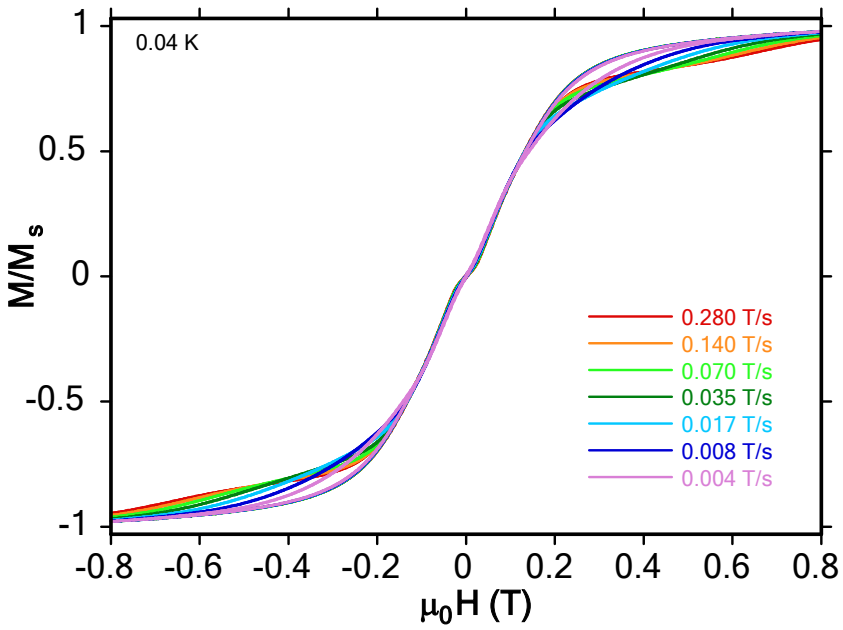

Figure S13. Single-crystal magnetization (*M*) vs. applied field measurements for complex $[(H_2O)NiLGd(H_2O)LNi(H_2O)]CF_3SO_3)_3$ at 0.04 K for several field sweep rates. *M* is normalized to its saturation value at 1.4 T.

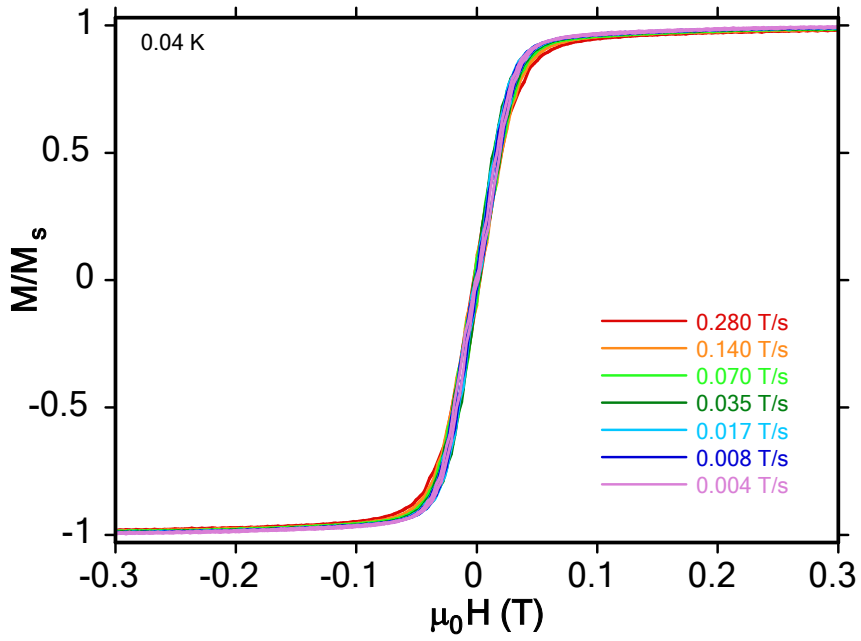

Figure S14. Single-crystal magnetization (*M*) vs. applied field measurements for complex **4** at 0.04 K for several field sweep rates. *M* is normalized to its saturation value at 1.4 T.

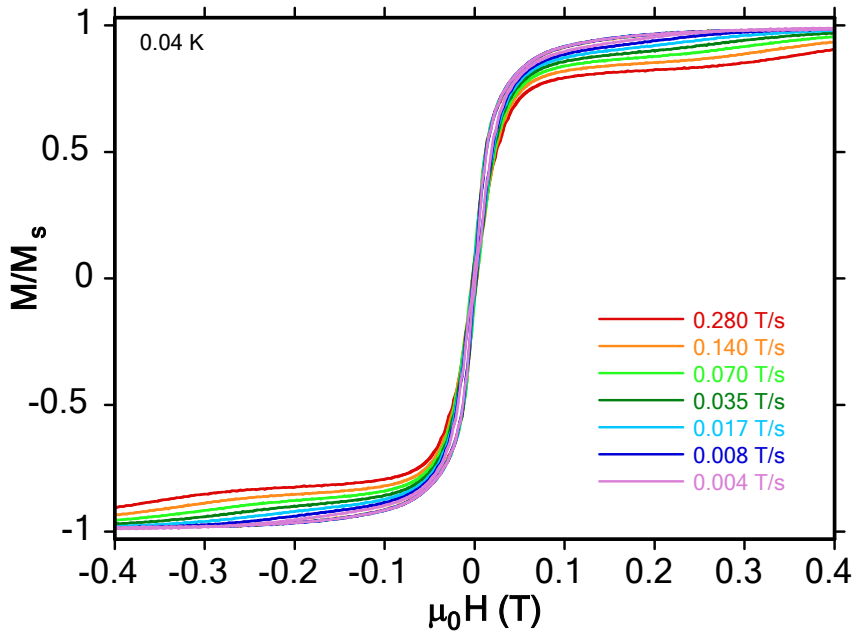

Figure S15. Single-crystal magnetization (*M*) vs. applied field measurements for complex **5** at 0.04 K for several field sweep rates. *M* is normalized to its saturation value at 1.4 T.

Table S1. Symmetry measures for the Ln ions in the studied complexes.

Complex		
9-coordinate Ln	CSAPR-9	TCTPR-9
1 Er	1.02	1.62
8 Y	2.84	2.86
8-coordinate Ln	TDD-8	
2 Gd	1.79	
3 Y	1.66	